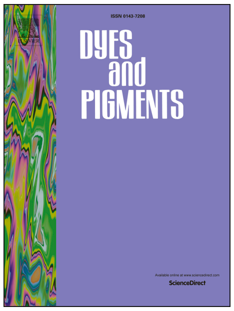

Two non-doped blue emitters for electroluminescent devices: Preparation, photophysics and electroluminescence

Jiarong Zhu, Ninghua Yin, Liheng Feng

PII: S0143-7208(16)30177-2

DOI: 10.1016/j.dyepig.2016.04.048

Reference: DYPI 5227

To appear in: *Dyes and Pigments*

Received Date: 25 March 2016

Revised Date: 27 April 2016

Accepted Date: 28 April 2016

Please cite this article as: Zhu J, Yin N, Feng L, Two non-doped blue emitters for electroluminescent devices: Preparation, photophysics and electroluminescence, *Dyes and Pigments* (2016), doi: 10.1016/j.dyepig.2016.04.048.

Two Non-doped Blue Emitters for Electroluminescent Devices: Preparation, Photophysics and Electroluminescence

Jiarong Zhu, Ninghua Yin, Liheng Feng*

School of Chemistry and Chemical Engineering, Shanxi University, Taiyuan, 030006, P.R. China.
E-mail address: lhfeng@sxu.edu.cn (L. Feng); Tel.:+86 351 7010904; Fax: +86 351 7011688.

Abstract: Two blue emitters, 2,7-bis(9-benzyl-9*H*-carbazol-2-yl)pyrene and 2,7-bis(4-(5-phenyl-1,3,4-oxadiazol-2-yl)phenyl)pyrene, were synthesized by a Suzuki coupling reaction. Photophysical studies show that the two emitters have excellent optical and electron transfer properties. The emission peaks of the two emitters are 430 nm and 439 nm with 87.5% and 68.6% fluorescence quantum yields in chloroform, respectively. The emitters both have good thermal stability (Td>330 ^{o}C, Tg>160 ^{o}C). Electrochemical Redox properties of the emitters were measured by cyclic voltammetry, and the highest occupied molecular orbital and the lowest unoccupied molecular orbital levels are in good agreement with the results of theoretical calculations. Additionally, non-doped blue organic light-emitting diodes with these emitters have been achieved with the Commission International de l'Éclairage (x,y) coordinates of (0.17, 0.11) and (0.16, 0.15) respectively, which are very close to the National Television System Committee standard blue. Remarkably, the performance of device A (2,7-bis(9-benzyl-9*H*-carbazol-2-yl) pyrene) offers balanced performance and without any significant disadvantages.

Keywords: blue emitter, electroluminescent devices, pyrene, carbazole, oxadiazole

1. Introduction

Organic light-emitting diodes (OLEDs) have been developed rapidly due to the advantages of the low drive voltage, high luminance and high efficiency [1-5]. Red, green and blue light plays a very important role in the full-color display, as they are the three primary colors. To date, green and red OLEDs materials have been widely reported [6-15]. Due to the low energy consumption lighting, white OLEDs materials have also been developed rapidly [16-22]. In comparison with other shades of OLED materials, it is difficult to obtain high-efficient blue or deep blue OLEDs because of the necessary wide band gaps. Hence, it is always a large challenge to design and achieve blue OLEDs. Based on these requirements, recently, the development speed of blue OLEDs is also very fast and many different types of blue OLEDs have been reported. Carbazole and its derivatives have been widely used as good hole-transport materials in the preparation of blue OLEDs [23-28]. Fluorene and its derivatives can be used as efficient blue emitters in the preparation of blue OLEDs [23, 28-35]. Moreover, chrysene derivatives [36], anthracene derivatives [37-39], triphenylamine derivatives [40], naphthalene derivatives [41,42] and other simple polymers [43-46] have also been used in OLEDs. Apart from these organic molecules, some metal complexes can be also used in OLEDs. Florian [47], Wong [48], Adachi [49] amongst other researchers have succeeded in using iridium (III) complexes to prepare blue OLEDs. Moreover, some other transition-metal complexes have also been successful in OLED applications [50].

Compared with other conjugated aromatic compounds, the pyrene functional group offers a high quantum yield, excellent electron mobility and hole-injection ability. However, pyrene itself has a strong tendency towards crystallization. Due to the π-π stack forming the excited molecule, its fluorescence emission may be red-shifted over

480 nm and with pyrene derived molecules it is difficult to form a stable amorphous thin film, which makes pyrene itself unsuitable for blue OLEDs [51,52]. Therefore, it is imperative to modify pyrene structures with some specific functional groups. Rao and his coworkers have successfully appended an electron transport group to blue emitting pyrene derivatives. But the CIE_y of these compounds are over 0.2, and the thermal stability of these compounds are not good [53]. Mullen and his coworkers successfully prepared a dark blue emitter with pyrene and carbazole units, but the brightness of corresponding OLED is low (<1000 $cd \cdot m^{-2}$) [24]. Tao and his coworkers also prepared pyrene derivatives with 4-(2,2-diphenyl-vinyl)phenyl group [54]. The performances of combined devices are good, but they are not deep blue OLEDs. Similarly, other researchers also designed and developed some pyrene derivatives as blue OLEDs materials [55-58]. These obtained pyrene emitters have their own particular characteristics, but more or less have their disadvantages, such as either larger CIE_y, lower brightness or emitting violet light. Additionally, hole-transfer and electron-injection properties of emitters are two important parameters for OLEDs materials.

Based on the current case, the aim of our work is to achieve excellent blue emitters with hole-transfer or electron-injection groups. Hence, we designed and synthesized two novel pyrene emitters with 9-benzyl-9-*H*-carbazole (hole-transfer group) and 2,5-diphenyl-1,3,4-oxadiazole (electron-injection group), respectively. The test results of photophysical and electroluminescence properties display that the two compounds as emitters of OLEDs emit blue light. Noticeably, the device based on 2,7-bis(9-benzyl-9*H*-carbazol-2-yl)pyrene (BCP) emitter has good properties including higher brightness, pure blue light and good stability.

2. Experimental

2.1 Materials

Unless otherwise stated, all chemical reagents were obtained from commercial suppliers and were used without further purification. The following reagents: Pd(dppf)Cl_2, bis(pinacolato)diboron, *N*-bromosuccinimide, phosphoryl chloride, $Pd(PPh_3)_4$, 4-bromobenzoyl chloride, phenylhydrazine, *N*-benzylcarbazole and 1,6-dibromopyrene were all purchased from Aldrich (Steinheim, Germany).

2.2 Characterization

^1H NMR and ^{13}C NMR were measured on a Bruker ARX400 spectrometer with chemical shifts reported as ppm (TMS as an internal standard). The UV-Vis absorption and fluorescence emission spectra were taken on a HITACHI UH5300 and F-4600 spectrophotometers, respectively. The excitation and emission slit widths were both 5.0 nm. High-resolution mass spectra (HRMS) were acquired on an Agilent 6510 Q-TOF LC/MS instrument (Agilent Technologies, Palo Alto, CA) equipped with an electrospray ionization (ESI) source. IR-spectroscopy measurements were performed on a FTIR8400S spectrophotometer, using KBr pellets. Elemental analyses were measured on a EuroVector EA3000 elemental analyzer. The glass transition temperatures of compounds were determined by DSC using a DSC-Q10 instrument under a nitrogen atmosphere. The decomposition temperature corresponding to 5 % weight loss was detected using a Perkine Elmer Pyris 1 TGA thermal analyzer. The melting points of compounds were recorded on a WRS-3 instrument with a 3 °C/min heating rate. Cyclic voltammetry (CV) measurements were determined on a three-electrode AUTOLAB (model PGSTAT30) workstation in a solution of Bu_4NClO_4 (0.1 M) in acetonitrile at a scan rate of 50 mV/s at room temperature.

2.3 Device fabrication

The multilayer OLEDs were fabricated by vacuum-deposition method. Organic layers were fabricated by high-vacuum (5×10^4 Pa) thermal evaporation onto a glass (3 cm×3 cm) substrate percolated with an ITO layer, which was used as anode. The hole-transfer layer (HTL) was poly(3,4-ethylenedioxythiophene):poly(styrenesulfonate) (PEDOT: PSS). The electron-blocking layer was 4,4-bis(*N*-carbazolyl)-1,10-biphenyl (CBP). The emitting layer was BOP and BCP, respectively. The electron-transport layer (ETL) was 1,3,5-tris(*N*-phbenylbenzimidazol-2-yl) benzene (TBPI). The cathode was LiF/Al. All organic layers were sequentially deposited. Thermal deposition rates for organic materials, LiF and Al were 0.5 $Å\cdot s^{-1}$, 0.5$\cdot$ $Å\ s^{-1}$and 1.0 $Å\cdot s^{-1}$, respectively. The active areas of these devices were 9 mm^2. The electroluminescent spectra were measured on a Hitachi MPF-4 fluorescence spectrometer. The voltage-current density characteristics of OLEDs were recorded on Keithley 2400 Source Meter. The characterization of luminance-voltage was measured with a 3645 DC power supply combined with a 1980 A spot photometer and was recorded simultaneously. All measurements were done at room temperature.

2.4 Synthesis procedures of BCP and BOP

Compounds of 9-benzyl-3-(4,4,5,5-tetramethyl-1,3,2-dioxaborolan-2-yl)-9*H*-carbazole and 2-phenyl-5-(4-(4,4,5,5-tetramethyl-1,3,2-dioxaborolan-2-yl)phenyl)-1,3,4-oxadiazole were prepared according to the previous reported works [59-61].

2.4.1 2,7-bis(9-benzyl-9H-carbazol-2-yl)pyrene (BCP)

A mixture with 1,6-dibromopyrene (0.9 g, 2.5 mmol), 9-benzyl-3-(4,4,5,5-tetramethyl-1,3,2-dioxaborolan-2-yl)-9*H*-carbazole (1.92 g, 5.0 mmol) in dioxane (50.0 mL) and 2.0 M K_2CO_3 (10.0 mL) was stirred for 30 min at room temperature under nitrogen atmosphere. Then, $Pd(PPh_3)_4$ (0.1 g) catalyst was quickly added to the suspension and heated to 110 ^oC for 48 h under nitrogen atmosphere. The reaction mixture was cooled to room temperature, poured into the ice water (200 mL), filtered and then purified by column chromatography on silica gel with dichloromethane /petroleum ether (1/1, v/v) as the eluant to afford BCP as faint yellow solids (1.149g 64.5 %), m.p. 275-277 °C. ^{1}H NMR (CDCl$_3$, 400 MHz) δ 8.42 (s, 2H), 8.34-8.31 (d, *J*=12.0 Hz, 2H), 8.26-8.22 (m, 4H), 8.19-8.06 (m, 6H), 7.76-7.73 (t, *J*=6.0, 6.0 Hz, 2H), 7.67-7.59 (t, *J*=8.0, 8.0 Hz, 2H) , 7.56-7.45 (m, 4H), 7.36-7.04 (m, 10H), 5.65 (s, 4H). ^{13}C NMR (CDCl$_3$, 100 MHz) δ 141.21, 140.03, 138.56, 137.18, 132.50, 130.23, 128.87, 128.33, 127.57, 126.54, 126.12, 125.42, 123.24, 122.39, 120.56 , 119.44, 108.70, 46.83. IR (KBr, υcm^{-1}):(arene C-H) 3083, 3030; (aliphatic C-H) 2920, 2856; (C=C, Ar) 1625, 1601; (C-N, Ar) 1477, 1466. Element Analysis for $C_{54}H_{36}N_2$ (Mol. Wt.: 712.90) calcd.: C, 90.98; H, 5.09; found: C 91.12; H 4.98. HRMS-ESI for $C_{54}H_{36}N_2$ (m/z) 713.53 [M+1].

2.4.2 2,7-bis(4-(5-phenyl-1,3,4-oxadiazol-2-yl)phenyl)pyrene (BOP)

The BOP was synthezied according to the above method. The crude produce was purified by column chromatography on silica gel with ethyl acetate/dichloromethane (1/12, v/v) as the eluant to afford BOP as a pale fawn solid (0.905 g 56.3 %), m.p. 285-287 °C, respectively. ^{1}H NMR (CDCl$_3$, 400 MHz) δ 8.50 (d, *J*=6.4 Hz, 2H), 8.41 (d, *J*=4.8, 2H), 8.39-8.25 (m, 8H), 8.14 (d, *J*=12.0 Hz, 2H), 8.03 (d, *J*=8.0 Hz, 2H), 7.89 (d, *J*=8.0 Hz, 4H), 7.62 (m, 6H). ^{13}C NMR (CDCl$_3$, 100 MHz) δ 164.71, 135.34, 131.77, 129.08, 127.00, 126.06, 125.97, 123.89, 84.25, 25.03. IR (KBr, υcm^{-1}): (arene C-H) 3043; (C=C, Ar) 1612, 1630; (C=N) 1546; (C-O-C) 1078, 1296. Element Analysis for $C_{44}H_{26}N_4O_2$ (Mol. Wt.: 642.72) calcd.: C, 82.23; H, 4.08; N, 8.72; found: C, 82.48; H, 4.51; N, 8.64; HRMS-ESI for $C_{44}H_{26}N_4O_2$ (m/z): 643.48 [M+1].

3. Results and discussion

3.1 Synthesis and photophysical properties of BCP and BOP

The synthetic routes used to prepare blue emitters BCP and BOP were showed in Scheme 1. The two compounds also were synthesized by Suzuki coupling reaction between 1, 6-dibromopyrene and carbazole boric acid ester or oxadiazoles boric acid ester in the presence of palladium catalyst with 64.5 % and 56.3 % yields, respectively [59-61]. The structures of BCP and BOP were characterized and verified by ^{1}H NMR, ^{13}C NMR, high resolution mass (HRMS), IR-spectroscopy and elemental analysis (EA). Due to larger rigid conjugated structures of BCP and BOP, they have poor solubility in routine organic solvents, for example ethyl acetate, acetone, ethanol, methanol, diethyl ether, etc.

The photophysical properties of BCP and BOP were studied by UV-Vis absorption and fluorescence emission techniques. **Fig. 1** gives the absorption and emission spectra of BCP and BOP in $CHCl_3$. As can be seen from **Fig. 1**, BOP and BCP have similar absorption and emission peaks, and the peaks are very close. The λ_{max} of absorption peaks of BCP and BOP are 370 nm and 372 nm, respectively. Accordingly, the emission peaks of BCP and BOP are 430 nm and 435 nm, respectively. The energy gaps (E_g) of BCP and BOP were calculated by the empirical equation [E_g=1240/λ_{abs}]. The energy gaps (Eg) of BCP and BOP are 3.33 eV and 3.35 eV, which are very close to the theoretical calculation results 3.34 eV and 3.33 eV, respectively. Using quinine sulfate in 0.10 M sulfuric acid as the reference, the fluorescent quantum yields (Φ) of BCP and BOP in $CHCl_3$ are 87.5 % and 68.6 % in chloroform, respectively. These data indicate that the two compounds can be used as potential blue emitting materials because they have suitable blue emitting range.

The solvent effects of BCP and BOP were tested by the fluorescence instrument in different organic solvents (**Table *S1***). As can be seen from the **Table *S1***, the maximum emission wavelengths (λ_{em}) of BCP and BOP are both gradually red-shifted with increase of solvent polarity. The result may be explained by the following reason: the polarity of excited state always is smaller than the ground state because of the π-π* transition of molecules. Thus, the interaction between the excited state and polar solvent is larger than the interaction between ground state and polar solvent. That is to say, the energy difference between the ground state and excited state becomes small with the increase of solvent polarity. So the emission peaks of BCP and BOP are red-shifted.

3.2 Thermal properties of BCP and BOP

Good thermal stability of emitter materials plays very important in device application. The thermal stabilities of BOP and BCP were evaluated by thermal gravimetric analysis (TGA) with a 5.0 °C/min heating rate and differential scanning calorimetry (DSC) under nitrogen atmosphere. Due to their large molecular masses and rigid structures, both compounds showed good thermal stability. The decomposition temperatures (Td, 5 % weight loss) of BOP and BCP are 353 ºC and 333 ºC with the glass transition temperatures 164 ºC and 170 ºC (**Fig. 2**), respectively. These results indicate that BOP and BCP have good stable thermal properties and high glass transition temperatures, which will contribute to the device performance (longevity).

3.3 Electrochemical properties

Using cyclic voltammetry (CV) with a saturated calomel electrode as the reference electrode, we studied the electrochemical properties of BCP and BOP. Under N_2 atmosphere, using 0.10 M tetrabutylammonium perchlorate as the supporting electrolyte, the electrochemical properties of BCP and BOP were studied. ***Fig. S1 and Fig. S2*** give the electrochemical properties of BOP and BCP, respectively. There is an oxide peak and a reversible reduction peak in the entire electrochemical window of

BOP (***Fig. S1***). The initial oxidation potential is around +0.59 eV, which comes from the oxidation of the pyrene core and the reversible reduction. And, the reversible reduction peak is around -1.11 eV, which results from electron injection into the vacant *p*-orbital of BOP. That is to say, the electron distribution of LUMO is mainly on 2,5-diphenyl-1,3,4-oxadiazole moiety, which indicates that BOP can be used as a good electron-transfer material. The HOMO energy level is -5.33 eV, which can be calculated by the empirical equation [HOMO=-(Eox+4.5+0.24) eV]. The HOMO level indicates that the electron distribution is mainly in the pyrene moiety. The energy gap (E_g) of BOP is 3.33 eV, which is obtained by the equation [E_g=1240/λ_{abs}]. The LUMO energy level is -2.00 eV, which is calculated by the HOMO and E_g. Similarly, the HOMO, LUMO level and E_g of BCP were obtained by the same calculation methods (***Fig. S2***). The HOMO, LUMO and E_g of BCP are -5.35 eV, -2.02 eV and 3.33 eV, respectively. The electron distributions of HOMO and LUMO for BCP are mainly on the pyrene core. These results indicate that the emission of BCP mainly comes from the excited state of pyrene core.

3.4 Theoretical calculation

Theoretical calculations have been widely used in many research fields and can effectively provide a reasonable qualitative indication of the excitation and emission properties of a conjugated molecule [62, 63]. Using density functional theory (DFT), the geometries and electron density distributions of the HOMO and LUMO energy levels of BOP and BCP. Under the DFT/B3LYP/6-31G (d, p) level with using Gaussian 09 software the geometry in the ground state was optimized. The geometries and electron density distributions of the HOMO and LUMO energy levels of BOP and BCP were calculated by density functional theory (DFT) in **Fig. 3**. As can be seen from **Fig. 3**, the HOMO level of BOP is -5.33 eV and the electron density is mainly distributed on the pyrene moiety. The LUMO level is -2.00 eV and electron density is mainly distributed on the oxadiazole moiety. The HOMO and LUMO of BCP is -5.33 eV and -1.99 eV, respectively. But the electron distributions of HOMO and LUMO for BCP are both mainly on the pyrene moiety. In addition, complete localization of the HOMO and LUMO is essential for efficient hole and electron transport and the prevention of reverse energy transfer as well [64].

3.5 Electroluminescence Devices

In order to evaluate BOP and BCP as potential luminescent materials in OLEDs, multilayers non-doped OLEDs with configurations of A:ITO/PEDOT:PSS(50 nm)/BCP(30 nm)/CBP(5 nm)/TPBI(30 nm)/LiF(1 nm)/Al(200 nm) and B:ITO/ PEDOT:PSS(50 nm)/BOP(30 nm)/CBP(5 nm)/TPBI(30 nm)/LiF(1 nm)/Al(200 nm) were fabricated. The electroluminescence (EL) spectra of device A and B are displayed in **Fig. 4** and **Fig.** ***S3***. The emission peaks of BCP and BOP are 450 nm and 440 nm respectively. According to the EL spectra, the electroluminescence chromaticity coordinates (CIE) of BCP and BOP are (0.17, 0.11) and (0.16, 0.15), respectively. The results suggest that the two compounds afford deep blue coloured OLEDs materials and the diode constructed using BCP is much deeper blue than that using BOP (**Fig. 5**). From the EL spectra it can also be found that the emission peaks of BCP and BOP are red-shifted about 10 nm and 15 nm in contrast with their PL emission peaks in $CHCl_3$. Along with the increase of the voltage, there are almost no changes of the EL emission wavelengths of device A and device B, which indicates that both device A and device B are very stable.

The voltage-luminance and voltage-current density curves of device A and device B are depicted in the **Fig. 6(a)** and **(b)**, respectively. While the current density-efficiency and luminance-power efficiency curves are listed in ***Fig. S4-S5***. Based on these experiment results, we can find the turn-on voltage, maximum luminance, maximum current efficiency and maximum power efficiency of device **A** are 4.6 V, 1975 cd·m^{-2} (at 9.5 V), 1.08 cd A^{-1}(at 6.2 V) and 0.628 lm·W^{-1}(at 5.2 V), respectively. Similarly, the turn-on voltage, maximum luminance, maximum current efficiency and maximum power efficiency of Device **B** are 4.8 V, 1282 cd·m^{-2} (at 9.5 V), 0.73 cd·A^{-1}(at 7.0 V) and 0.328 lm·W^{-1}(at 7.0 V), respectively. Compared to the electroluminescence data of device **A** with device **B**, the performance of device **A** is superior to device **B**. The experimental data indicate that all aspects of device **A** are well suited with the application of deep blue OLEDs. It should be pointed out that the EL performances were obtained in non-optimized test devices under ordinary laboratory conditions. We believe that the performance of devices will be improved by optimizing the structures of devices, the layer thickness and process conditions.

4. Conclusion

In summary, we have successfully synthesized and characterized two deep blue-light emitters (BCP and BOP) by Suzuki coupling reactions. The advantages of photophysical and electroluminescence properties of the two emitters are as follows: 1) they are both new OLEDs materials with good π-electron delocalization and conjugation features; 2) The CIEs of BCP and BOP are (0.17, 0.11) and (0.16, 0.15), which indicates that both of them are deep blue-light emitting materials; 3) They are comprised of luminophor (pyrene) and electron-transfer group (oxadiazole) or hole-transport group (carbazole), respectively; 4) Owing to the rigid structures, they have good thermal stabilities; 5) The performance of device A is balanced and without obvious disadvantages. In other words, the emitter with hole-transfer group (BCP) is better than with electron-transport group (BOP) in device application. With the optimization of structures and layers thickness, the properties of devices will be improved and may meet commercial requirements.

Acknowledgment

The work described in this paper was supported by the National Nature Science Foundation (No. 21571116 and 21371110), the Youth Science Foundation of Shanxi Province (No. 2014021006) and the Program for the Outstanding Innovative Teams of Higher Learning Institutions of Shanxi (2013).

Appendix. Supplementary data

Other fluorescence spectroscopy (PDF) associated with this article can be found in the online version, at doi:

References

[1] Tang CW, Vanslyke SA. Organic electroluminescent diodes. Appl Phys Lett 1987; 51: 913-5.

[2] Chen SF, Deng LL, Xie J, Peng L, Xie LH, Fan QL et al. Recent developments in top-emitting organic light-emitting diodes. Adv Mater 2010; 22: 5227-39.

[3] Burroughes JH, Bradley DDC, Brown AR, Marks RN, Friend RH, Burn PL et al. Light-emitting diodes based on conjugated polymers. Nature 1990; 37: 539-41.

[4] Zhu MR, Yang CL. Blue fluorescent emitters: design tactics and applications in organic light-emitting diodes. Chem Soc Rev 2013; 42: 4963-76.

[5] Reineke S, Lindner F, Schwartz G, Seidler N, Walzer K, Sseml B, et al. White organic light-emitting diodes with fluorescent tube efficiency. Nature 2009; 459: 234-8.

[6] Bucinskas A, Volyniuk D, Danyliv Y, Grazulevicius JV, Baryshnikov G, Minaev B, et al. N-annelated perylenes as effective green emitters for OLEDs. RSC Adv 2015; 5: 78150-9.

[7] Cho YJ, Jeon SK, Chin BD, Yu ES, Lee JY. The design of dual emitting cores for green thermally activated delayed fluorescent material. Angew Chem Int Ed 2015; 54: 5201-4.

[8] Zhao QH, Zhang WY, Fan ZX, Li JJ, Chen XM, Luo GG, et al. Synthesis and characterization of high triplet energy polyfluorene bearing m-tetraphenylsilane segment as a polymer host for green phosphorescent polymer light emitting diodes. Synth Met 2015; 204: 70-5.

[9] Jankus V, Abdullah K, Griffiths GC, Al-Attar H, Zheng YH, Bryce MR, et al. The role of exciplex states in phosphorescent OLEDs with poly (vinylcarbazole) (PVK) host. Org Electron 2015; 20: 97-102.

[10] Zhang S, Xue LS, Jing YM, Liu X, Lu GZ, Liang X, et al. 1-(N-phenylamino)naphthalene oligomers as novel hole transport materials for highly efficient green electrophosphorescence. Dyes Pigments 2015; 118: 1-8.

[11] Feng YS, Li P, Zhuang XM, Ye KQ, Peng T, Liu Y, et al. A novel bipolar phosphorescent host for highly efficient deep-red OLEDs at a wide luminance range of 1000-10 000 cd/m^2. Chem Commun 2015; 51: 12544-47.

[12] Qin W, Lam JWY, Yang ZY, Chen SM, Liang GD, Zhao WJ, et al. Red emissive AIE luminogens with high hole-transporting properties for efficient non-doped OLEDs. Chem Commun 2015; 51: 7321-24.

[13] Zhou L, Li LJ, Jiang YL, Cui RZ, Li YN, Zhao XS, et al. Rare earth complex as electron trapper and energy transfer ladder for efficient red iridium complex based electroluminescent devices. ACS Appl Mater Interfaces 2015; 7: 16046-53.

[14] Liu J, Miao JS, Wu HB. Efficient solution-processed double-layer red OLEDs based on a new europium complex with a carbazole group. Luminescence 2015; 30: 393-6.

[15] Kim JW, Yoo S, Kang JS, Lee SE, Kim YK, Yu HH, et al. Color stable white phosphorescent organic light emitting diodes with red emissive electron transport layer. J Appl Phys 2015; 117: 245503.

[16] Farinola GM, Ragni R. Electroluminescent materials for white organic light emitting diodes. Chem Soc Rev 2011; 40: 3467-82.

[17] Schwartz G, Pfeiffer M, Reineke S, Walzer K, Leo K. Harvesting triplet excitons from fluorescent blue emitters in white organic light-emitting diodes. Adv Mater 2007; 19: 3672-6.

[18] Wu YS, Hwang SW, Chen HH, Lee MT, Shen WJ, Chen CH. Efficient white organic light emitting devices with dual emitting layers. Thin Solid Films 2005; 488: 265-9.

[19] Kamtekar KT, Monkman AP, Bryce MR. Recent advances in white organic light-emitting materials and devices. Adv Mater 2010; 22: 572-82.

[20] Sun Y, Forrest SR. High-efficiency white organic light emitting devices with three separate phosphorescent emission layers. Appl Phys Lett 2007; 91: 263503.

[21] Schwartz G, Fehse K, Pfeiffer M, Walzer K, Leo K. Highly efficient white organic light emitting diodes comprising an interlayer to separate fluorescent and phosphorescent regions. Appl Phys Lett 2006; 89: 083509.

[22] Andrade BWD, Holmes RJ, Forrest SR. Efficient organic electrophosphorescent white-light-emitting device with a triple doped emissive layer. Adv Mater 2004; 16: 624-8.

[23] Wei Y, Wang WJ, Huang YT, Wang BC, Chen WH, Wua SH, et al. Blue fluorescent dihydro-indenoindene derivatives with unusual low oxidation potentials as multifunctional OLED materials. J Mater Chem C 2014; 2: 1779-82.

[24] Chercka D, Yoo SJ, Baumgarten M, Kim JJ, Mullen K. Pyrene based materials for exceptionally deep blue OLEDs. J Mater Chem C 2014; 2: 9083-6.

[25] Sasabe H, Toyota N, Nakanishi H, Ishizaka T, Pu YJ, Kido J. 3,3′-bicarbazole-based host materials for high-efficiency blue phosphorescent OLEDs with extremely low driving voltage. Adv Mater 2012; 24: 3212-7.

[26] Lin SL, Chan LH, Lee RH, Yen MY, Kuo WJ, Chen CT, et al. Highly efficient carbazole-p-dimesitylborane bipolar fluorophores for nondoped blue organic light-emitting diodes. Adv Mater 2008; 20: 3947-52.

[27] Liang ZQ, Chu ZZ, Yang JX, Yuan CX, Tao XT, Zou DC. X-shaped tetra-substituted pyrenes: synthesis, photophysics, and electroluminescence. Synth Met 2011; 161: 1691-8.

[28] Huang J, Yang X, Wang JY, Zhong C, Wang L, Qin JG, et al. New tetraphenylethene-based efficient blue luminophors:aggregation induced emission and partially controllable emitting color. J Mater Chem 2012; 22: 2478-84.

[29] Li ZF, Jiao B, Wu ZX, Liu P, Ma L, Lei XL, et al. Fluorinated 9,9′-spirobifluorene derivatives as host materials for highly efficient blue organic light-emitting devices. J Mater Chem C 2013; 1: 2183-92.

[30] Tang C, Liu F, Xia YJ, Lin J, Xie LH, Zhong GY, et al. Fluorene-substituted pyrenes-novel pyrene derivatives as emitters in nondoped blue OLEDs. Org Electron 2006; 7: 155-62.

[31] Loy DE, Koene BE, Tompson ME. Thermally stable hole-transporting materials based upon a fluorine core. Adv Funct Mater 2002; 12: 245-49.

[32] Chiang CL, Tseng SM, Chen CT, Hsu CP, Shu CF. Influence of molecular dipoles on the photoluminescence and electroluminescence of dipolar spirobifluorenes. Adv Funct Mater 2008; 18: 248-57.

[33] Tang S, Liu MR, Lu P, Xia H, Li M, Xie ZQ, et al. A molecular glass for deep-blue organic light-emitting diodes comprising a 9,9′-spirobifluorene core and peripheral carbazole groups. Adv Funct Mater 2007; 17: 2869-77.

[34] Chen SF, Tian Y, Peng JH, Zhang HR, Feng XJ, Zhang HX, et al. Synthesis and characterization of arylamino end-capped silafluorenes for blue to deep-blue organic light-emitting diodes (OLEDs). J Mater Chem C 2015; 3: 6822-30.

[35] Liu C, Gu Y, Fu Q, Sun N, Zhong C, Ma DG, et al. Nondoped deep-blue organic light-emitting diodes with color stability and very low efficiency roll-off: solution-processable small-molecule fluorophores by phosphine oxide linkage. Chem Eur J 2012; 18: 13828-35.

[36] Chung YH, Sheng L, Xing X, Zheng L., Bian MY, Chen ZJ, et al. A pure blue emitter (CIEy≈0.08) of chrysene derivative with high thermal stability for OLED. J Mater Chem C 2015; 3: 1794-8.

[37] Wu CL, Chang CH, Chang YT, Chen CT, Chen CT, Su CJ. High efficiency non-dopant blue organic lightemitting diodes based on anthracene-based fluorophores with molecular design of charge transport and red-shifted emission proof. J Mater Chem C 2014; 2: 7188-200.

[38] Wu CH, Chien CH, Hsu FM, Shih P, Shu CF. Efficient non-doped blue-light-emitting diodes incorporating an anthracene derivative end-capped with fluorene groups. J Mater Chem 2009; 19: 1464-70.

[39] Zhu MR, Wang Q, Gu Y, Cao XS, Zhong C, Ma DG, et al. Efficient deep-blue emitters comprised of an anthracene core and terminal bifunctional groups for nondoped electroluminescence. J Mater Chem 2011; 21: 6409-15.

[40] Li WJ, Yao L, Liu HC, Wang ZM, Zhang ST, Xiao R, et al. Highly efficient deep-blue OLED with an extraordinarily narrow FHWM of 35 nm and a y coordinate <0.05 based on a fully twisting donor–acceptor molecule. J Mater Chem C 2014; 2: 4733-6.

[41] Hu JY, Pu YJ, Nakata G, Kawata S, Sasabe H, Kido J. A single-molecule excimer-emitting compound for highly efficient fluorescent organic light-emitting devices. Chem Commun 2012; 48: 8434-36

[42] Oh HY, Lee CH, Lee S. Efficient blue organic light-emitting diodes using newly-developed pyrene-based electron transport materials. Org Electron 2009; 10: 163-9.

[43] Giovanella U, Botta C, Galeotti F, Vercelli B, Battiatoc S, Pasini M. Perfluorinated polymer with unexpectedly efficient deep blue electroluminescence for full-colour OLED displays and light therapy applications. J Mater Chem C 2013; 1: 5322-9.

[44] Gao ZQ, Li ZH, Xia PF, Wong MS, Cheah KW, Chen CH. Efficient deep-blue organic light-emitting diodes: arylamine substituted oligofluorenes. Adv Funct Mater 2007; 17: 3194-9.

[45] Bacher E, Bayerl M, Rudati P, Reckefuss N, Muller CD, Meerholz K, et al. Synthesis and characterization of photo-cross-linkable hole-conducting polymers. Macromolecules 2005; 38: 1640-7.

[46] Shu CF, Dodda R, Wu FI. Highly efficient blue-light-emitting diodes from polyfluorene containing bipolar pendant groups. Macromolecules 2003; 36: 6698-703.

[47] Kessler F, Watanabe Y, Sasabe H, Katagiri H, Nazeeruddin MK, Gratzel M, et al. High-performance pure blue phosphorescent OLED using a novel bis-heteroleptic iridium (III) complex with fluorinated bipyridyl ligands. J Mater Chem C 2013; 1: 1070-5.

[48] Zhou GJ, Ho CL, Wong WY, Wang Q, Ma DG, Wang LX, et al. Manipulating charge-transfer character with electron-withdrawing main-group moieties for the color tuning of iridium electrophosphors. Adv Func. Mater 2008; 18: 499-511.

[49] Kawamura Y, Goushi K, Brooks J, Brown JJ, Sasabe H, Adachi C, et al. 100% Phosphorescence quantum efficiency of Ir(III) complexes in organic semiconductor films. Appl Phys Lett 2005; 86: 071104.

[50] Chi Y, Chou PT. Transition-metal phosphors with cyclometalating ligands: fundamentals and applications. Chem Soc Rev 2010; 39: 638-55.

[51] Mikroyannidis JA, Fenenko L, Adachi C. Synthesis and photophysical characteristics of 2,7-fluorenevinylene-based trimers and their electroluminescence. J Phys Chem B 2006; 110: 20317-26.

[52] Wu KC, Ku PJ, Lin CS, Shih HT, Wu FI, Huang MJ, et al. The photophysical properties of dipyrenylbenzenes and their application as exceedingly efficient blue emitters for electroluminescent devices. Adv Funct Mater 2008; 18: 67-75.

[53] Mallesham G, Swetha C, Niveditha S, Mohanty MEN, Babu J, Kumar A, et al. Phosphine oxide functionalized pyrenes as efficient blue light emitting multifunctional materials for organic light emitting diodes. J Mater Chem C 2015; 3: 1208-24.

[54] Liang ZQ, Chu ZZ, Zou DC, Wang XM, Tao XT. Novel 4-(2, 2-diphenyl-vinyl)-phenyl substituted pyrene derivatives as efficient emitters for organic light-emitting diodes. Organic Electronics 2012; 13: 2898-904.

[55] Chan KL, Lim JPF, Yang XH, Dodabalapur A, Jabbour GE, Sellinger A. High-efficiency pyrene-based blue light emitting diodes: aggregation suppression using a calixarene 3D-scaffold. Chem Commun 2012; 4: 5106-08.

[56] Wang ZQ, Liu CL, Zheng CJ, Wang WZ, Xu C, Zhu M, et al. Efficient violet non-doped organic light-emitting device based on a pyrene derivative with novel molecular structure. Organic Electronics 2015; 23: 179-185.

[57] Zhao ZJ, Chen SM, Lam JWY, Lu P, Zhong YC, Wong KS, et al. Creation of highly efficient solid emitter by decorating pyrene core with AIE-active tetraphenylethene peripheries. Chem Commun 2010: 46: 2221-3.

[58] Jeltsch KF, Lupa G, Weitz RT. Materials depth distribution and degradation of a fIrpic based solution-processed blue OLED. Org Electron 2015; 26: 365-70.

[59] Chen W, Wunderlich B. Nanophase separation of small and large molecules. Macromol Chem Phys 1999; 200: 283-311.

[60] Ponce MB, Cabrerizo FM, Bonesi SM, Balsells RE. Synthesis and electronic spectroscopy of bromocarbazoles direct bromination of *N*- and *C*-substituted carbazoles by *N*-bromosuccinimide or a *N*-bromosuccinimide/silica gel system. Helv Chim Acta 2006; 89: 1123-39.

[61] Peng ZH, Bao ZN, Galvin ME. Polymers with bipolar carrier transport abilities for light emitting diodes. Adv Mater 1998; 10: 680-4.

[62] Belletete M, Morin JF, Leclerc M, Durocher GA. A theoretical, spectroscopic, and photophysical study of 2,7-carbazolenevinylene. J Phys Chem A 2005; 109: 6953-9.

[63] Becke AD. Density-functional thermochemistry. III. the role of exact exchange. J Chem Phys 1993; 98: 5648-52.

[64] Ge Z, Hayakawa T, Ando S, Ueda M, Akiike T, Miyamoto H, et al. Spin-coated highly efficient phosphorescent organic light-emitting diodes based on bipolar triphenylamine-benzimidazole derivatives. Adv Funct Mater 2008; 18: 584-90.

The figures and scheme captions

Scheme 1. The synthesis routes of BCP and BOP.

Fig. 1 The UV-vis absorption and fluorescence emission spectra of BCP and BOP in $CHCl_3$.

Fig. 2 TGA thermogram of BCP and BOP with a heating rate of 5 ^{o}C/min under nitrogen atmosphere, respectively.

Fig. 3 Molecular orbital surfaces of the HOMO and LUMO for BCP and BOP.

Fig. 4 The electroluminescence spectra of BCP and BOP in device A, (ITO/PEDOT:PSS/BCP/CBP/TPB/LiF/Al).

Fig. 5 The electroluminescence (CIE) chromaticity coordinates of BCP and BOP.

Fig. 6 (a) Plots of voltage versus luminance for blue-light emitting devices A and B, (b) Plots of voltage versus current density for blue-light emitting devices A and B, (ITO/PEDOT:PSS/BCP/CBP/TPB/LiF/Al; ITO/PEDOT:PSS/BCP/CBP/TPB/LiF/Al).

Scheme 1

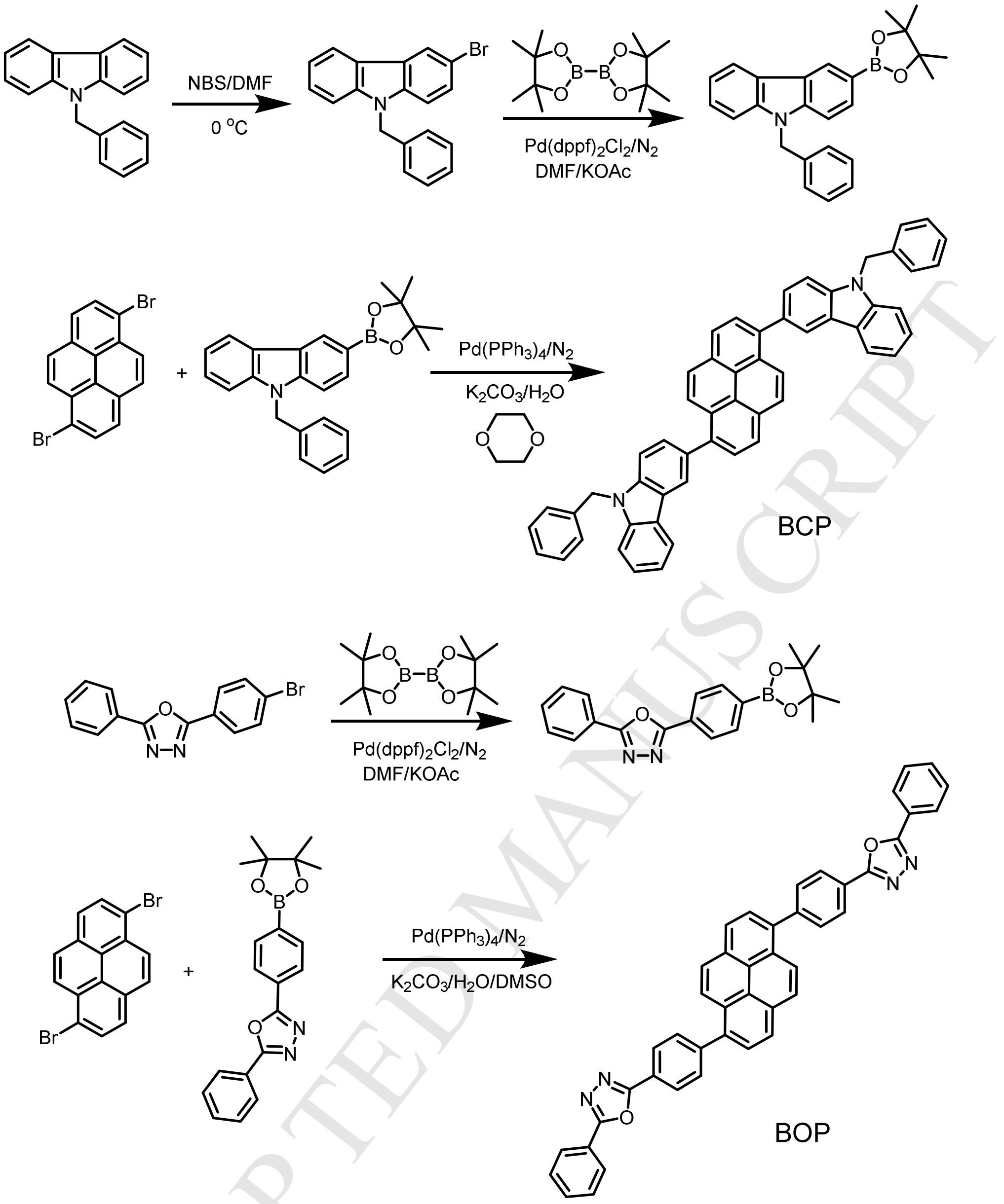
Br
NBS/DMF
0 °C
N
O
B
$Pd(dppf)_2Cl_2/N_2$
DMF/KOAc
$Pd(PPh_3)_4/N_2$
K_2CO_3/H_2O
BCP
$Pd(PPh_3)_4/N_2$
$K_2CO_3/H_2O/DMSO$
BOP

Fig. 1

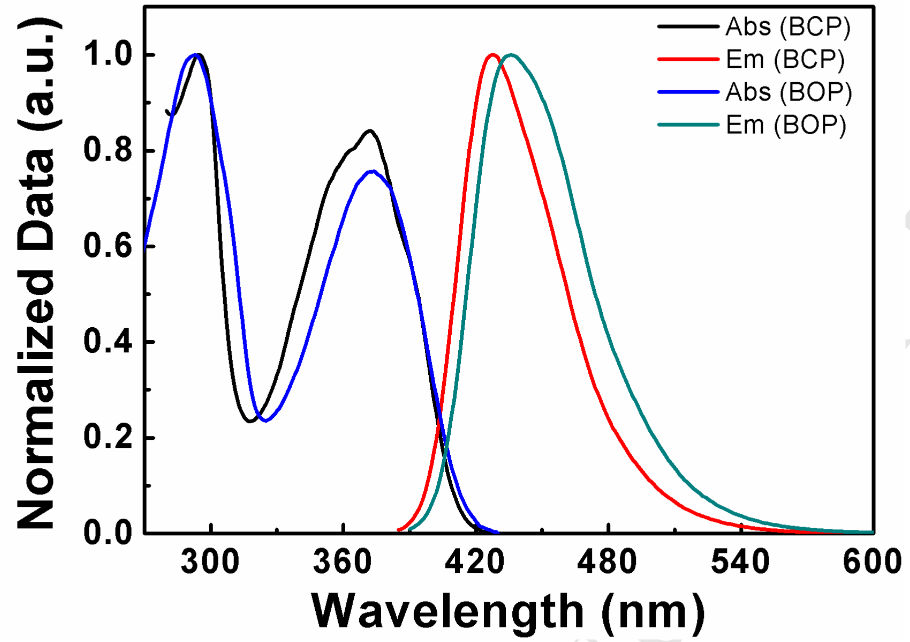
Abs (BCP)
Em (BCP)
Abs (BOP)
Em (BOP)
Normalized Data (a.u.)
0.0
0.2
0.4
0.6
0.8
1.0
300
360
420
480
540
600
Wavelength (nm)

Fig. 2

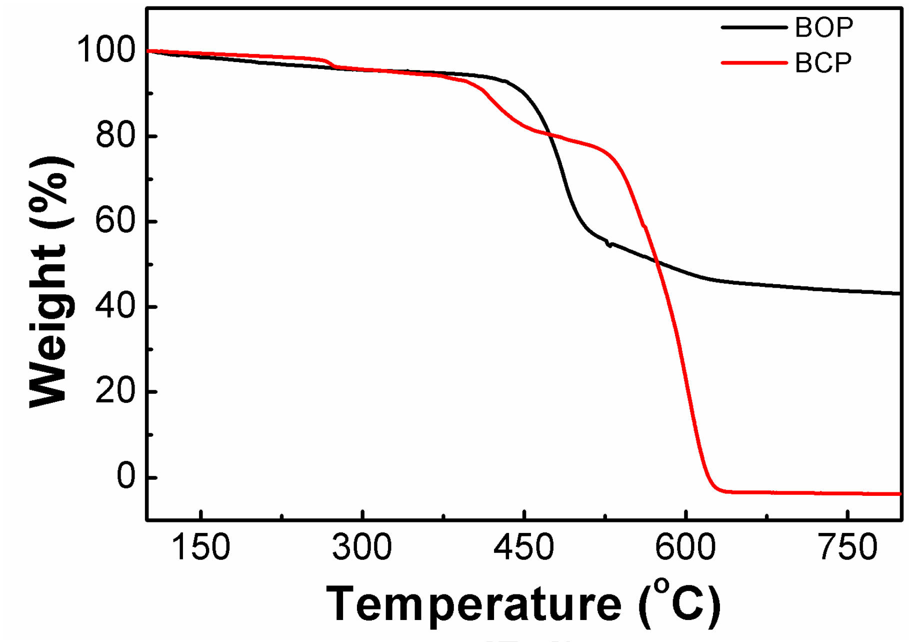
BOP
BCP
Weight (%)
100
80
60
40
20
0
150
300
450
600
750
Temperature (°C)

Fig. 3

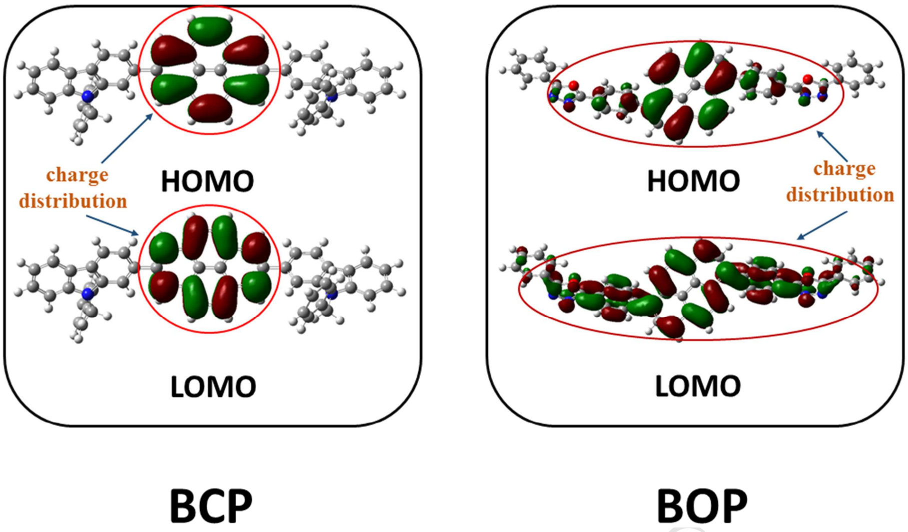
charge distribution
HOMO
LOMO
BCP
HOMO
charge distribution
LOMO
BOP

Fig. 4

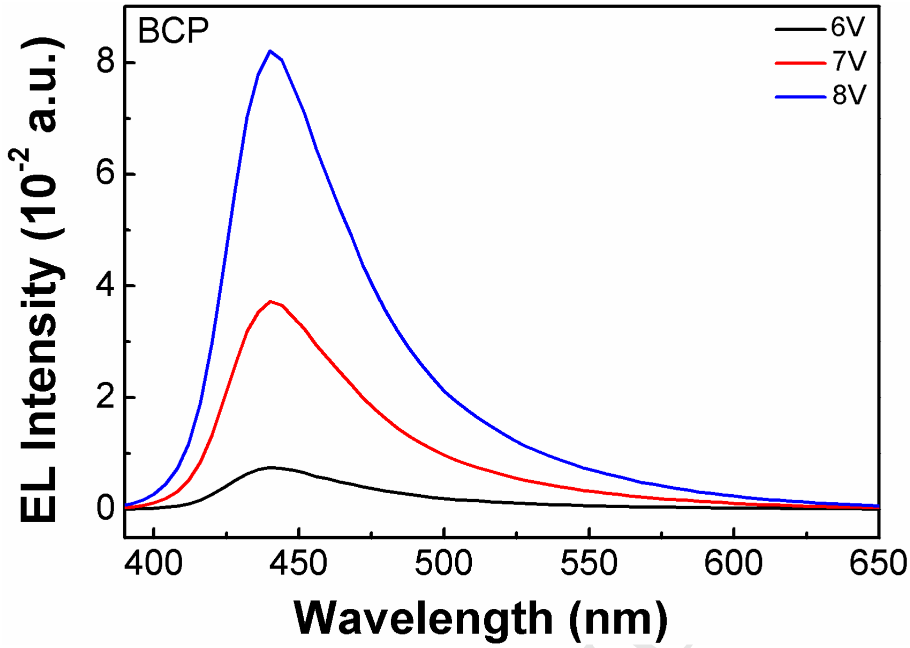
BCP
6V
7V
8V
EL Intensity (10^{-2} a.u.)
0
2
4
6
8
400
450
500
550
600
650
Wavelength (nm)

Fig. 5

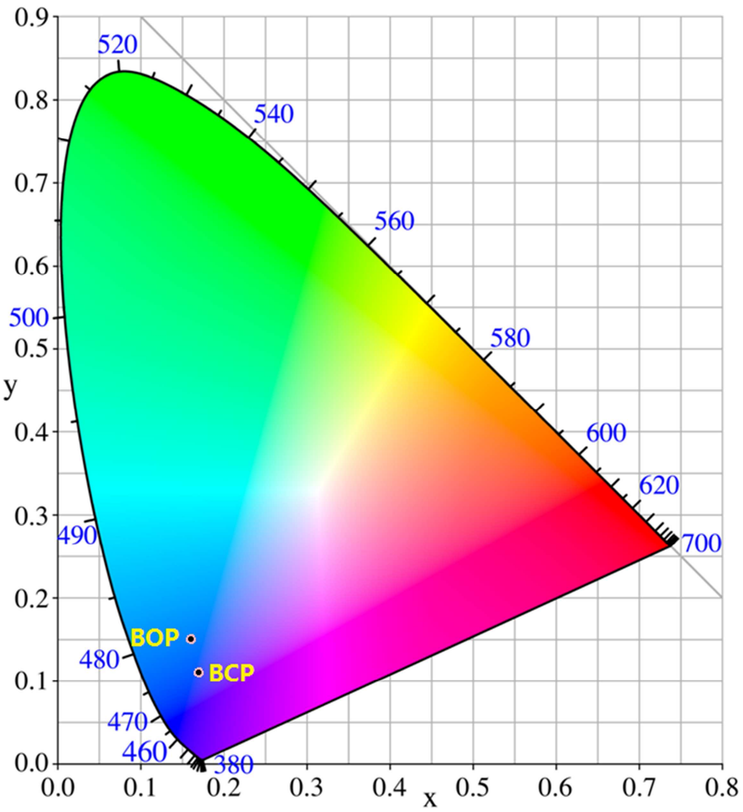
0.9
0.8
0.7
0.6
0.5
0.4
0.3
0.2
0.1
0.0
y
0.0
0.1
0.2
0.3
0.4
0.5
0.6
0.7
0.8
x
520
540
560
580
600
620
700
500
490
480
470
460
380
BOP
BCP

Fig. 6

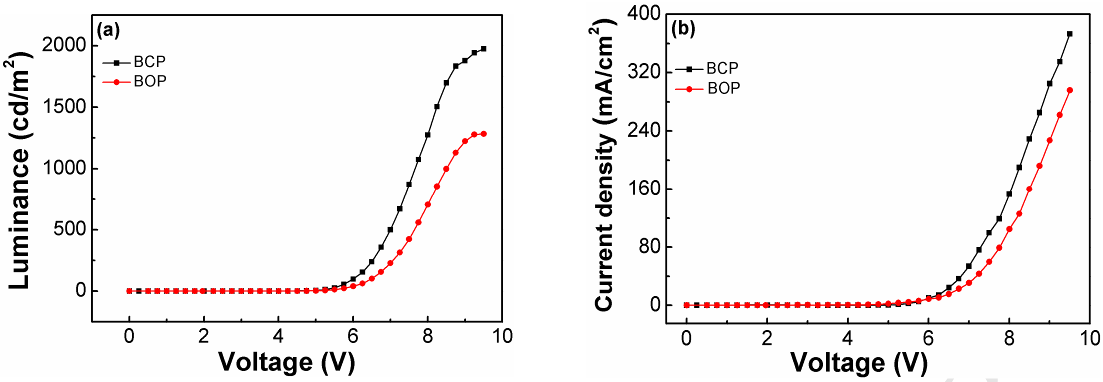
(a)
Luminance (cd/m^2)
2000
1500
1000
500
0
BCP
BOP
0
2
4
6
8
10
Voltage (V)
(b)
Current density (mA/cm^2)
400
320
240
160
80
0
BCP
BOP
0
2
4
6
8
10
Voltage (V)

Two Non-doped Blue Emitters for Electroluminescent Devices: Preparation, Photophysics and Electroluminescence

Jiarong Zhu, Ninghua Yin, Liheng Feng*

School of Chemistry and Chemical Engineering, Shanxi University, Taiyuan, 030006, P.R. China.

E-mail address: lhfeng@sxu.edu.cn (L. Feng); Tel.:+86 351 7010904; Fax: +86 351 7011688.

Highlights

Two novel blue emitting OLED materials were designed and synthesized.

These emitters exhibit good thermal stability and electron transfer properties.

The device with BCP emitter has good optical and electrical characteristics.